On the Governing Chemistry of Cellulose Hydrolysis in Supercritical Water

*Danilo A. Cantero, M. Dolores Bermejo and M. José Cocero**

High Pressure Processes Group, Department of Chemical Engineering and Environmental Technology, University of Valladolid, Prado de la Magdalena s/n, 47011 Valladolid, SPAIN.

FAX: +34-983423013. *E-mail: mjcocero@iq.uva.es

Keywords: Biomass • Ionic Product • Kinetic • Sugars • Water Chemistry

Abstract

This article summarizes the recent efforts in the High Pressure Processes Group labs at UVa regarding the fundamentals of biomass hydrolysis in pressurized water medium. At extremely low reaction times (0.02 s), cellulose was hydrolyzed in supercritical water (400ºC and 25 MPa) obtaining a sugars yield higher than 95% $w \cdot w^{-1}$ while 5-HMF yield was lower than 0.01% $w \cdot w^{-1}$. When the reaction times was increased up to 1 s, the main product was glycolaldehyde (60% $w \cdot w^{-1}$). Independently of the reaction time, the yield of 5-HMF was always lower than 0.01% $w \cdot w^{-1}$. In order to evaluate the reaction pathway and mechanism of plant biomass in pressurized water, several parameters (temperature, pressure, reaction time and reaction medium) were studied for different biomasses (cellulose, glucose, fructose and wheat bran). It was considered that the reactions of glucose isomerization to fructose as well as fructose dehydration to 5-HMF take place via proton or hydroxide anion association. So, their concentration was taken into account as reagent concentration in the reaction evaluations. It was found that the proton and hydroxide anion concentration in the medium due water dissociation is the determining factor in the selectivity of the process. The reaction of glucose isomerization to fructose and its further dehydration to produce 5-HMF are highly dependent on ions concentration. By increasing pOH/pH, these reactions were minimized allowing the control of 5-HMF production. At this condition, the retro-aldol condensation pathway was enhanced instead of isomerization/dehydration pathway.

INTRODUCTION

The biomass exploitation as raw material is growing as an alternative for the sustainable production of fuels and chemicals[1]. Cellulose is one of the main compounds of biomass, representing the most abundant biopolymer[2]. An important challenge in the processing of cellulosic biomass is to hydrolyze the β1-4 glucose-glucose bond producing a stream of sugars with low concentration of byproducts, by using an efficient process[3-5]. This sugars streams could be further transformed in valuable chemical like pyruvaldehyde, glycolaldehyde[6-9], 5-hydroxymetylfurfural (5-HMF)[10, 11], organic acids or poly-alcohols[12, 13]. Acid and enzymatic hydrolysis of cellulose are two conventional methods that need long treatment times (>3 h) to obtain a poor-selective product (<60% w/w)[14, 15]. The use of ionic liquids as solvent and reaction medium has been intensively studied due to the possibility of dissolve cellulose making it more 'accessible' to the hydrolysis reaction[16, 17]. However, this kind of process take at least 3 h of hydrolysis to obtain a selectivity near to 30% w/w of reducing sugars[16]. These processing methods require large reaction times (hours), which will demand big reactors at the scaling up time. The use of pressurized water is an alternative as reaction medium for the processing of cellulosic biomass in a one-step fast process. Total hydrolysis of cellulose can be achieved in 0.02 s of reaction time in a supercritical water medium producing a stream of water soluble sugars with low concentration of derived products (<2% w/w)[18, 19]. This kind of process represents an advantageous intensification that will reduce the energetic and equipment requirements in the scaling up.

Cellulose depolymerization in hot pressurized water have been done in different kind of reactors (batch, semi-batch and continuous) at different temperatures and pressure, with or without catalysts[20]. The yield of sugars after biomass hydrolysis is enhanced by using supercritical water reactors operated in a continuous mode at high temperature and low reaction times[19, 21]. The combination of these two parameters is crucial for obtaining high

yields in sugars. At long reaction times, the sugars are derived and; at low reaction temperatures several side reactions take place producing many compounds. In fact, it was observed that some reactions are avoided at supercritical conditions. Especially attention should be played to the formation of 5-HMF. The production of 5-HMF from cellulose in pressurized water is highly dependent on reaction temperature. In Figure 1 it is shown several experimental results of cellulose hydrolysis in pressurized water from 300ºC to 400ºC at different pressures along reaction times.

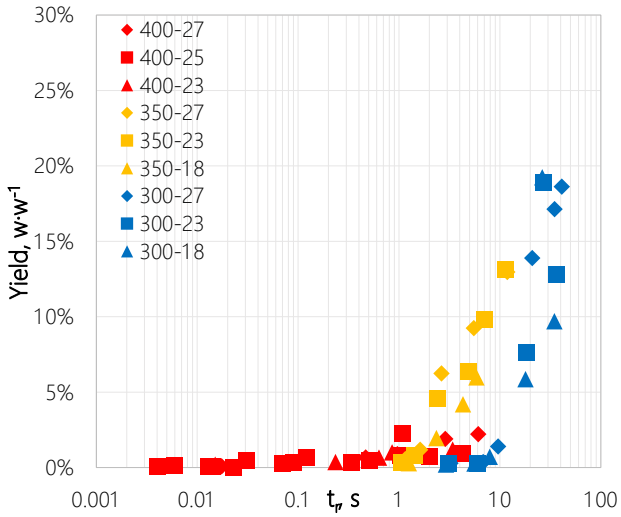

Figure 1. 5-HMF yield from cellulose hydrolysis in pressurized water along reaction time. Experiment temperature: red: 400ºC; yellow: 350ºC and; blue: 300ºC. Experiment pressure: (diamonds) 27 MPa; (squares) 25 / 23 MPa and; (triangles) 23 / 18 MPa.

It can be observed that 5-HMF production was faster, but the yield lower, when the reaction temperature was increased from 300ºC to 350ºC. The reaction time was reduced from 40 s to 10 s by increasing the reaction temperature. This behavior was expected and it follows the Arrhenius law. However, an expected behavior was detected by increasing the reaction temperature over the critical point of water, the production of 5-HMF was highly avoided. Although this behavior was previously detected in bibliography[6, 7, 18, 22-35], a clear and quantitative explanation has not been developed yet. The different discovered behaviors

71 can be classified in three main groups. (1) The maximum amount of 5-HMF from cellulose in
72 pressurized water without catalyst is produced at temperatures lower than 300ºC [18, 23, 29, 31, 33].
73 An increase in temperature benefits the retro aldol condensation reactions of fructose[33]. (2)
74 The production of 5-HMF is enhanced increasing the availability of protons (H^+) in the
75 reaction medium by adding acids[25-28, 30]. (3) The production of 5-HMF is enhanced in a
76 pressurized water medium when pressure is increased at a constant temperature[6, 7].
77 The aim of this work was to study the reactions of cellulose hydrolysis, focusing in the 5-
78 HMF production from sugars. The yields were analyzed from a chemical point of view of the
79 reaction pathway. Several reactions were run in order to obtain accurate data. Cellulose
80 hydrolysis was experimented at 300ºC, 325ºC, 350ºC, 375ºC and 400ºC at 25 MPa of
81 pressure. Also, the pressure effect was tested at 300ºC, 350ºC and 400ºC between 18 and 27
82 MPa. The studies were also conducted analyzing glucose and fructose hydrolysis in
83 pressurized water between 300ºC and 400ºC at 25 MPa. Finally, the results were contrasted
84 with the products obtained from wheat bran hydrolysis in supercritical water. A reaction
85 pathway was developed and a novel kinetic model was tested for understanding the behavior
86 of glucose and fructose reaction in supercritical water.

87 **METHODS**

88 **Materials**

89 The cellulose (99%) used in the experiments was purchased from VWR. Glucose (99%)
90 and fructose (99%) used as starting biomass in the experiments were purchased from Sigma.
91 Wheat bran was supplied by a local supplier. Distilled water was used as reaction medium in
92 the experiments. The standards used in HPLC (High Performance Liquid Chromatography)
93 analysis were: cellobiose (+98%), glucose (+99%), fructose (+99%), glyceraldehyde (95%),

pyruvaldehyde (40%), glycolaldehyde dimer (99%), levulinic acid (+99%), 5-HMF (99%) purchased from Sigma.

Analysis

The carbon content of the liquid products was determined by total organic carbon (TOC) analysis with Shimadzu TOC-VCSH equipment. The composition of the liquid products was determined by High Performance Liquid Chromatography (HPLC) analysis. The HPLC column used for the separation of the compounds was Sugar SH-1011 Shodex at 50ºC using H_2SO_4 (0.01 N) as mobile phase with a flow rate of 0.8mL/min. A Waters IR detector 2414 was used to identify and quantify the sugars and their derivatives. An UV-Vis detector was used to determine the 5-hidroxy-methyl-furfural (5-HMF) concentration at a wavelength of 254nm. The selectivity of each compound (Si) was calculated as the ratio of: compound carbon composition (Xc) multiplied by compound concentration (Ci) and total carbon at the reactor inlet (TC). Si=Ci Xc/TC.

Experimental Facility

The experiments were carried out in a continuous pilot plant able to work at temperatures up to 425ºC and pressures up to 30 MPa. A schematic diagram of the process is shown in Figure 2. Two streams continuously fed a micro reactor: a cellulose stream and supercritical water stream. Strict control of the reaction times was achieved by a combination of three factors: (1) rapid heating by supercritical water injection of the cellulose suspension stream, (2) rapid cooling by sudden depressurization down to atmospheric pressure and ~100ºC using a micro metering valve able to stand temperatures up to 425 ºC, and (3) selection of a series of tubular reactors of different volumes accurately determined. The volume of the used reactors varied from 0.12 ml to 64.5 ml, which in combination with flows between 1 $g \cdot s^{-1}$ and 2 $g \cdot s^{-1}$, and having into account the density of water at the experimented conditions, gives

reaction times of 0.004 s to 40 s. A detailed description of the experimental setup was developed in Supporting Information. Although the reactor is fed by two streams (biomass and water), no extra water is needed in the process when the steady state is achieved. As it can be seen in Figure 2, after the reactor a flash chamber separator produces two streams: vapor (water) and liquid (sugars dissolved). The vapor is almost pure water that can be recirculated.

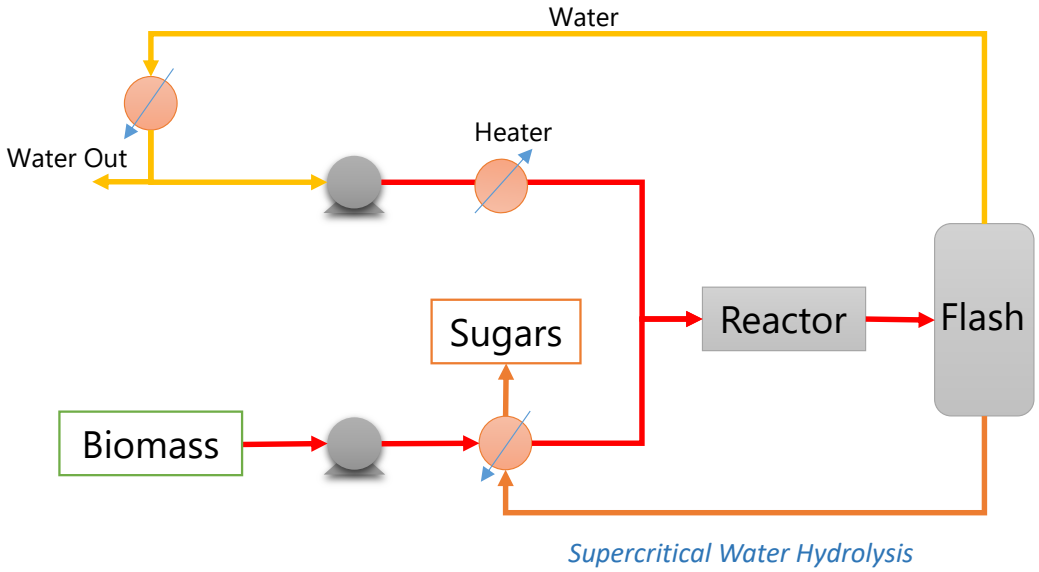

Figure 2. Schematic diagram of the supercritical water hydrolysis facility.

Reaction medium and reaction pathway

Supercritical water (SCW) is water at temperature and pressure values above its critical point (Tc=374ºC and Pc=22.1 MPa). In the surroundings of the critical point, the properties of water can be highly influenced by changing pressure and temperature. So, the identity of the medium can be modified without changing the solvent. The medium density represents the quantity of water per volume unit ($kg \cdot m^{-3}$); this is a measurement of water concentration, an important factor to take into account in the reactions where water participates as reagent or forming intermediate states[36]. Another important property of water as reaction medium is the ion product ($mol^2 \cdot kg^{-2}$), which represents how dissociated is water molecule (ion

concentration). If the molal concentration of OH^- (square root of ionic product) is multiplied by density, the molar concentration of protons or hydroxide anions in the medium is obtained. This concentration parameter includes both, the variations in water volume and its dissociation. The concentration of OH^- (which is the same for H^+) in the surroundings of the critical point of water is plotted in Figure 3.

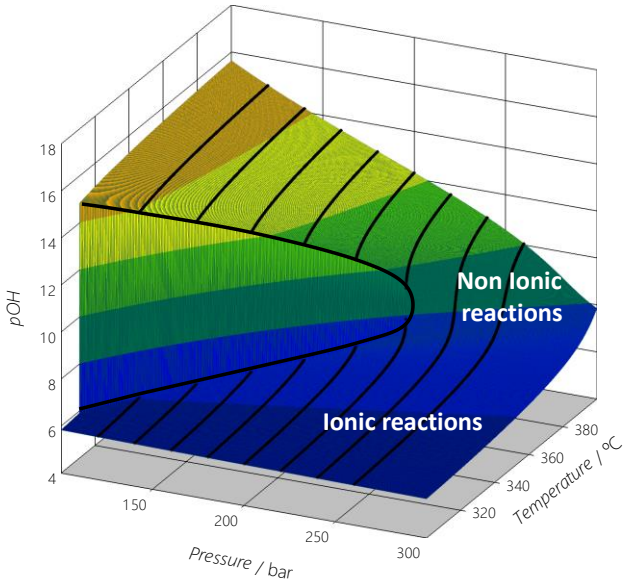

Figure 3. Hydroxyl concentration ($mol \cdot L^{-1}$) along temperature and pressure. pOH=-log(|OH^-|)=pH [37, 38]. Water density was calculated according the IAPWS industrial formulation[37], while the molal ionic product of water was calculated following 'International Formulation of Ionic Product of Water Substance'[38].

Important changes in the identity of the medium can be obtained if temperature and pressure are changed at the same time. For example, the density of water at 300ºC and 27 MPa is around 750 $kg \cdot m^{-3}$; this value can be decreased to 130 $kg \cdot m^{-3}$ if the conditions are modified to 400ºC and 23 MPa. The H^+/OH^- concentration varies six orders of magnitude in the neighborhood of the critical point allowing the possibility of working with markedly different reaction mediums. The H^+/OH^- concentration at 300ºC and 23 MPa is around $2 \cdot 10^{-6}$ $mol \cdot L^{-1}$ which means that the medium has high concentration of ions ([H^+] and [OH^-]) favoring the ionic reactions[6, 39-41]. The H^+/OH^- concentration will take a value of $5.5 \cdot 10^{-12}$

153 mol·L^{-1} if the temperature and pressure are changed to 400ºC and 23 MPa; this reaction
154 medium would favor radical reactions [42].

155 The reactions were assumed to follow the reaction pathway shown in Schema 1. This
156 reaction pathway was built following the schemas developed in literature[23]. The reaction of
157 glucose isomerization occurs via ring-opening and keto-enol tautomerism. These reactions
158 take place forming transition states with OH^- or H^+. Also, fructose dehydration takes place
159 forming transition states incorporating H^+ (one per H_2O molecule lost) [43]. In order to identify
160 these reactions in Schema 1, the symbols OH^-/H^+ were added above the reaction arrow. The
161 production of glycolaldehyde was enhanced at supercritical conditions because the
162 hydroxide/proton concentration is highly decreased (pH=pOH=13) and so is the
163 concentration of fructose and its derived products. Although the reaction of glucose
164 isomerization is avoided at low concentration of hydroxide anions, fructose yield near to 10%
165 w·w^{-1} was obtained at supercritical conditions.

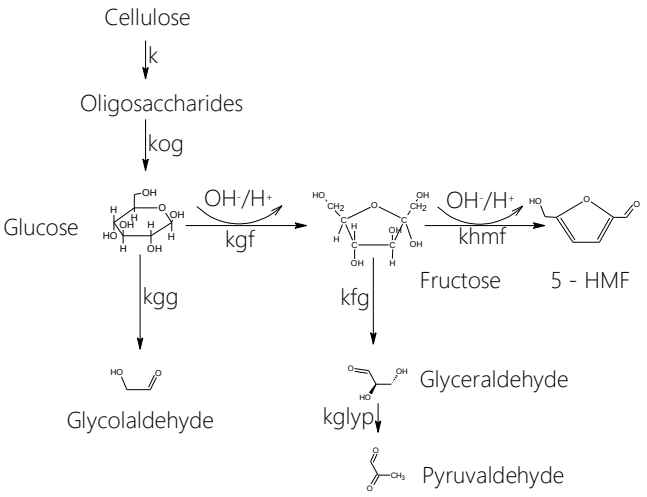

166

167 **Schema 1**. Main reaction pathway of cellulose hydrolysis in pressurized water.

168 As it is shown in Schema 1, fructose can follow two main reaction pathways: fructose
169 dehydration or retro aldol condensation. The second reaction was more benefited compared
170 to the first one obtaining, in this way, glyceraldehyde as main product from fructose. The

171 maximum quantity of 5-HMF was obtained working at 350ºC, 23 MPa (pH=pOH=6) at a
172 reaction time of 10 s. In those conditions the yield was around 15% $w \cdot w^{-1}$.

173 A reaction model was built considering cellulose as starting material. The concentration of
174 each compound shown in Schema 1 was calculated along reaction time. The difference
175 between the calculated concentrations and the experimental ones was minimized obtaining
176 the kinetic constant of the reactions[18]. Equation 1 shows the evolution of compound *i* along
177 reaction time, where n_i is the concentration of compound *i* ($mol \cdot L^{-1}$); *t* is time (s) and; k_{ji} (s^{-1})
178 is the kinetic constant of the reaction in which *j* reacts producing *i*.

179 $$\frac{dn_i}{dt} = \sum_1^n k_{ji} n_j - \sum_1^n k_{io} n_i \qquad (1)$$

180 In order to evaluate the medium effect in the selectivity, the model was solve in three
181 different ways; (1) considering only the concentration of cellulose and its derived products;
182 (2) considering also the water concentration and; (3) considering the concentration of
183 cellulose, its derived products and the protons or hydroxide anions concentration in the
184 reactions of glucose isomerization and fructose dehydration. Therefore, the concentration of
185 fructose was calculated according equation 2 or 3 in the resolution of model 2 or 3
186 respectively.

187 $$\frac{dn_f}{dt} = k_{gf} n_g n_w - k_{fh} n_f n_w - k_{fg} n_f \qquad (2)$$

188 $$\frac{dn_f}{dt} = k_{gf} n_g n_{OH-H} - k_{fh} n_f n_{OH-H} - k_{fg} n_f \qquad (3)$$

189 Where n_w is the water concentration ($mol \cdot L^{-1}$) and $n_{OH\text{-}H}$ is the concentration of OH^- or H^+
190 in the medium ($mol \cdot L^{-1}$).

RESULTS AND DISCUSSION

Sugars production from cellulose hydrolysis

The evolution of the sugars yield along reaction time can be seen in Figure 3 (see also Tables S.1 – S.10 in the Supporting Information). The best conditions to obtain soluble sugars (up to six glucose units) from the hydrolysis of cellulose were achieved by working at 400ºC with extremely short reaction times (0.015 s). When reaction time was increased, the sugars were hydrolyzed, so the yield decreased as it is shown in Figure 4. At 400ºC, the yield of soluble sugars was higher than 95% $w \cdot w^{-1}$. Similar methods of cellulose hydrolysis in pressurized water were developed in literature with selectivity of sugars lower than 77% w/w[21, 31, 44, 45]. The combination of supercritical water medium and the effective method of reaction time control presented in this work allow cellulose hydrolysis with high yield to sugars. This is because, at those conditions, the cellulose hydrolysis kinetic is fast enough while the glucose hydrolysis kinetics are slow enough to allow our reactor to stop the reactions after total hydrolysis and before glucose degradation[19]. It was observed that the cellulose hydrolysis would have a sugars yield between 80 – 98 % $w \cdot w^{-1}$ if the reaction time is between 0.015 – 0.2 s.

The best combination of conditions to obtain high yield of glycolaldehyde can be achieved by working at 400ºC and 23 MPa with a reaction time of 1 s. In those conditions the yield of glycolaldehyde was around 60% $w \cdot w^{-1}$. Sometimes, the production of 5-HMF is undesired, especially when a microorganism post process is needed[46]. At 400ºC, the 5-HMF production was highly avoided for all the studied pressures. Independently of the residence time (0.015 s for sugars or 1 s for glycolaldehyde) the concentration of 5-HMF was lower than 0.1% $w \cdot w^{-1}$.

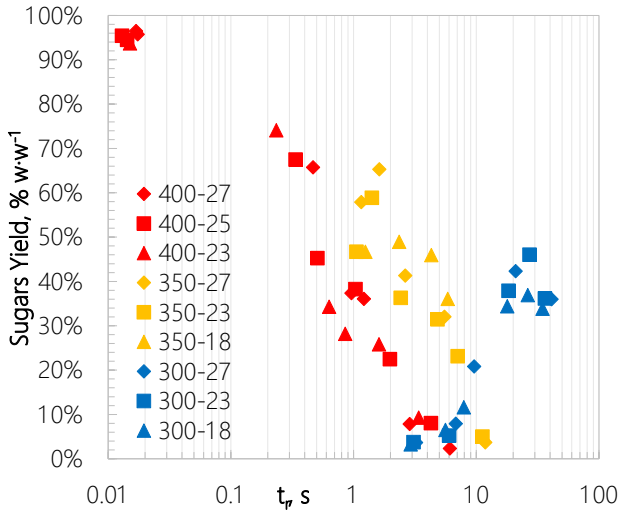

Figure 4. Sugars yield from cellulose hydrolysis in pressurized water along reaction time. Experiment temperature: red: 400ºC; yellow: 350ºC and; blue: 300ºC. Experiment pressure: (♦) 27 MPa; (■) 25 / 23 MPa and; (▲) 23 / 18 MPa.

Reaction model evaluation: cellulose hydrolysis at 25 MPa for different temperatures

The reaction pathway shown in Schema 1 was kinetically evaluated following the equations 1, 2 or 3. In Figure 5, the results for the three tested models are shown. The behavior of the reaction models will be compared by means of the results for the kinetic constants of fructose dehydration to 5-HMF. The obtained kinetic constants for the reaction rates *kog*, *kgg* and *kfg* obtained by the resolution of model 1 follow the Arrhenius law. However, the kinetics of glucose isomerization and fructose dehydration showed a break point near the critical point of water. As it can be observed in Figure 5-A, the model linearly predicts the kinetic constants of fructose dehydration at subcritical temperatures. However, near the critical point of water a break point in the kinetic was observed, which represents a deviation of the Arrhenius law. This phenomenon would be predicted because of the low concentration of 5-HMF in the products. Moreover, the concentration profiles for 5-HMF obtained at 400ºC were lower than the found at 350ºC or 300ºC (these concentration profiles can be seen in the Supporting Information). This deviation of the Arrhenius behavior suggests that another chemical effect

232 is not taken into account on the kinetic evaluation. In order to solve this problem, water or
233 ions concentration were counted as reagent concentration.

234 The reactions of glucose and fructose in near critical water are usually analyzed together
235 with the medium density in order to explain the selectivity of the process[4, 6, 7, 18].
236 Qualitatively, the theory of water transition states works well; if the medium density is low
237 the concentration of 5-HMF will be low. In order to quantify the participation of water in the
238 reaction, water concentration was added as reagent in the reaction of glucose isomerization
239 and fructose dehydration (model 2). Unfortunately, the kinetic constants obtained
240 considering water concentration as reagent did not follow the Arrhenius law at sub neither
241 supercritical water (Figure 5-B). Thus, from a quantitative point of view, the theory of water
242 transition states would not explain the low concentration of 5-HMF at supercritical
243 conditions. Finally, the kinetic constants of the whole reaction system followed the Arrhenius
244 law when model 3 was resolved (Figure 5-C).

245 The kinetic constants for cellobiose hydrolysis (*kh*), oligosaccharides hydrolysis (*kog*),
246 glucose isomerization to fructose (*kgf*), and glucose retro aldol condensation (*kgg*) are plotted
247 in Figure 6-A, 6-B, 6-C and 6-D respectively. It can be observed that the resolution of model
248 3 produce series of kinetic constants that follows the Arrhenius law for the whole system. The
249 dotted lines in Figure 6 represent the uncertainty of the kinetic constants considering the
250 experimental errors as well as the fitting errors. It is important to take into account the
251 dimension of the kinetic constant. For model resolution 3; *kh, kog* and *kgg* constants have the
252 same units (s^{-1}). However, kgf and khmf have second order units ($L \cdot mol^{-1} \cdot s^{-1}$). This is
253 because this two reaction were considered dependent of two reagents concentrations. In
254 addition, the obtained values of *kgf* and *khmf* were higher than the values of *kh*, *kog* and *kgg*.

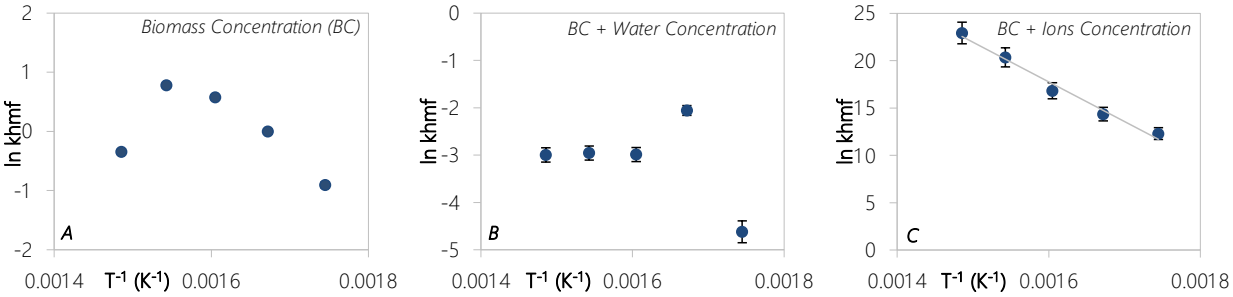

Figure 5. Kinetic constant for fructose dehydration to 5-HMF at 25 MPa and temperature between 300ºC and 400ºC. (A) Kinetic evaluation considering the biomass concentration as reagent concentration. (B) Kinetic evaluation considering the biomass concentration and water concentration as reagent concentration. (C) Kinetic evaluation considering the biomass concentration and ions concentration as reagent concentration. Error bars represent the experimental and fitting errors.

In order to describe the kinetic behavior along temperature for the different reactions, the activation energy (E_a) and the pre-exponential factor (ln ko) were calculated. These parameters are shown in Table 1 for all the kinetics fitted. It can be also observed in this table that the error in the Arrhenius parameters is around 5% considering the experimental and fitting uncertainty. Also, as it was previously analyzed for the kinetic constants of *kgf* and *khmf*, the values of the Arrhenius parameters for these constants were higher than for the others.

Table 1. Activation energy and pre-exponential factor of glucose reactions in pressurized water medium.

Kinetic	**Activation Energy**	**Error**	**Pre-exponential factor**	**Error**
kh (s^{-1})	90.4	4.5	17.4	0.9
kog (s^{-1})	145.5	6.1	28.6	1.2
kgf ($l \cdot mol^{-1} \cdot s^{-1}$)	566.3	34.1	127.3	6.6
kgg (s^{-1})	147.4	7.4	28.7	1.4
kfh ($l \cdot mol^{-1} \cdot s^{-1}$)	348.1	26.0	84.8	5.0

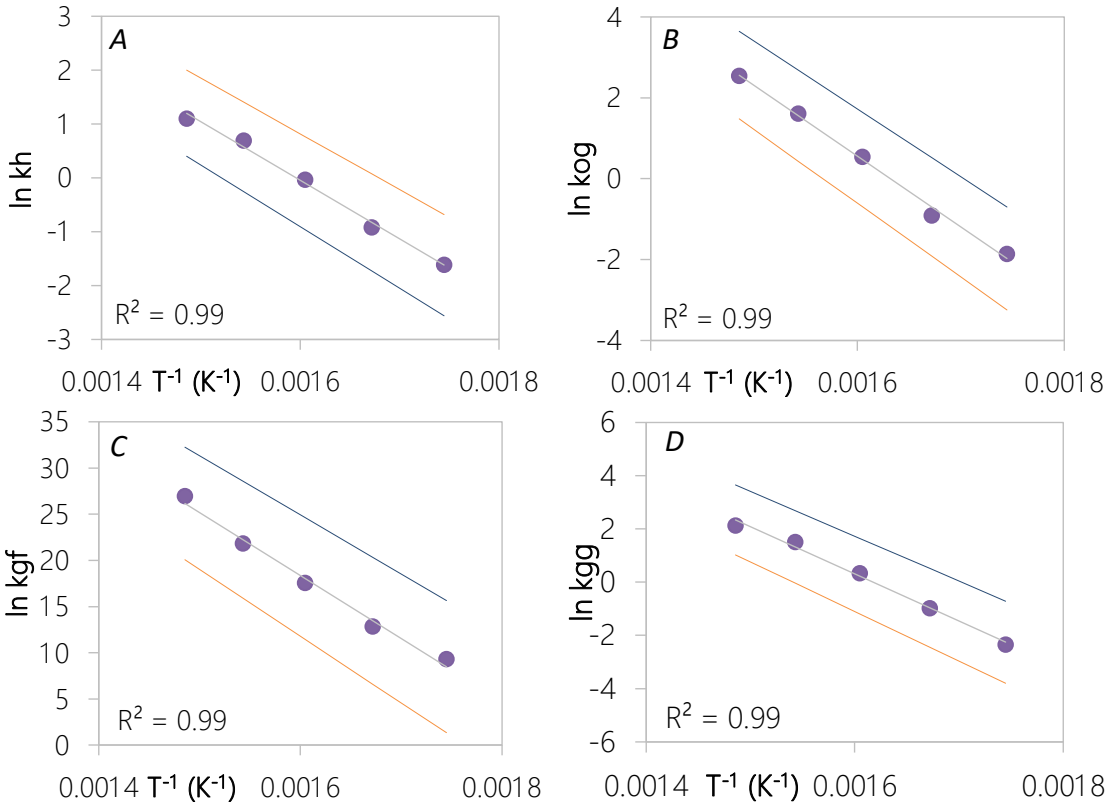

Figure 6. Kinetic constants for cellulose hydrolysis at 25 MPa and temperature between 300ºC and 400ºC. (***A***) Kinetic constants of cellobiose hydrolysis. (***B***) Kinetic constants of oligosaccharides hydrolysis. (***C***) Kinetic constants of glucose isomerization to fructose. (***D***) Kinetic constants of glucose retro-aldol condensation. Dotted line: uncertainty of the kinetics behavior.

Reaction model evaluation: cellulose hydrolysis at different pressures and temperatures

The evaluation of the reaction model was also tested for the reactions of cellulose hydrolysis at different pressures and temperatures. The cellulose hydrolysis was experimented at 300ºC (18, 23 and 27 MPa), 350ºC (18, 23 and 27 MPa) and 400ºC (23, 25 and 27 MPa). In Figure 7-A it can be seen the comparison of the three model results. Once again, the outcomes of models 1 and 2 did not follow the Arrhenius law. The fructose dehydration kinetics followed the Arrhenius law when model three was used to solve the

kinetics system. Although the results shown in Figure 6-A correspond to 27 MPa series, the results of Model 3 follow the Arrhenius law for all the experimented pressures, as it is shown in Figure 7-B. It should be taken into account that the experiments were always done in pressurized liquid or supercritical phase. This is because the series at 18 MPa was only experimented at 300ºC and 350ºC.

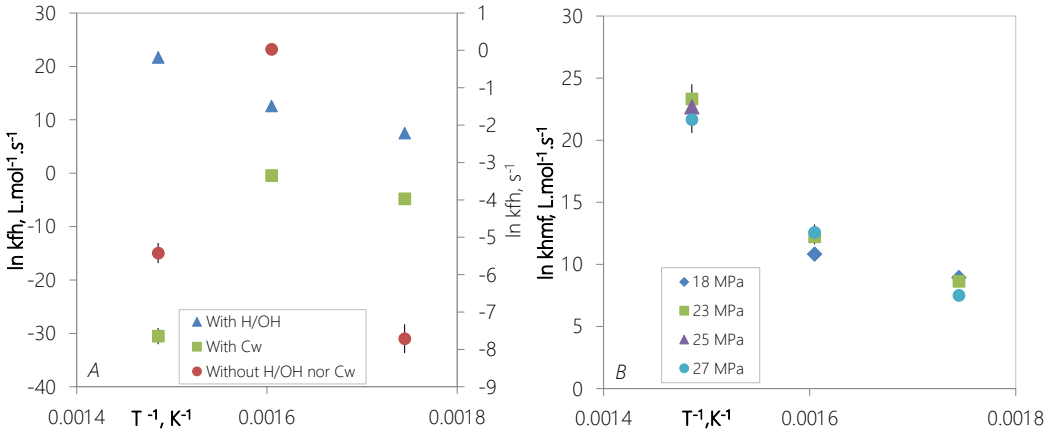

Figure 7. (***A***) Kinetic constant of fructose dehydration considering OH^- concentration (triangles), considering water concentration (squares) and non-considering OH^- nor water concentration (circles). Pressure= 27MPa. (***B***) Kinetic constant of fructose dehydration considering OH^- concentration at: 27 MPa (circles); 25 MPa (squares); 23 MPa (triangles) and 18 MPa (diamonds). Error bars represent the experimental and fitting errors.

Reaction model evaluation: glucose hydrolysis at 25 MPa for different temperatures

The reaction pathway and the kinetic model developed in section 3, 4 and 5 were also tested analyzing the glucose reactions in pressurized water. Glucose hydrolysis reactions were experimented at 25 MPa of pressure at temperature around the critical point of water (350, 385 and 400ºC), where the change in the ionic product of water is the highest. As it was expected, the obtained kinetic constants follow the Arrhenius law when the concentration of ions was considered as reagent concentration (model 3).

The reaction mechanism proposed in this work was tested in three different ways: cellulose hydrolysis at constant pressure changing temperature, cellulose hydrolysis changing pressure and temperature, and glucose hydrolysis at constant pressure changing temperature near the critical point of water. For the three situations, the kinetic constants of glucose hydrolysis reactions follow the Arrhenius parameters when the ions concentration of the medium was taken into account. In addition, the kinetics constants of glucose isomerization and fructose dehydration took similar order of magnitude for the different analyzed situations.

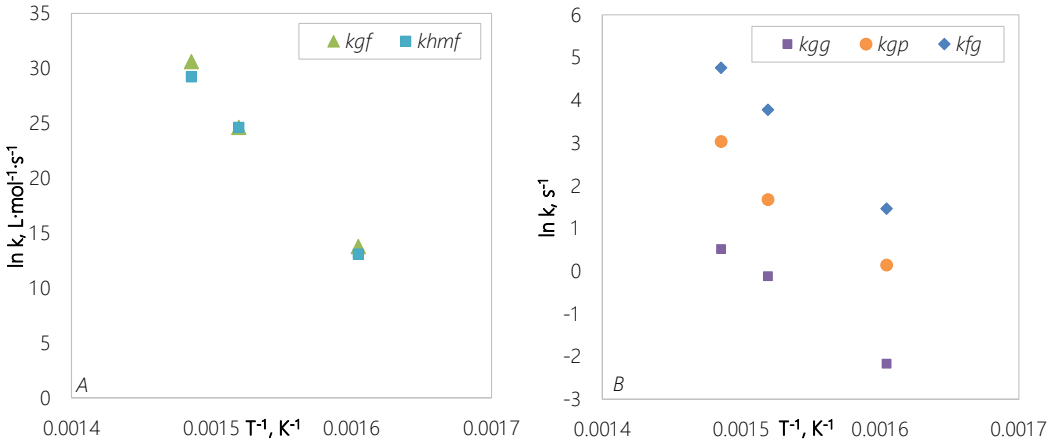

Figure 8. Glucose hydrolysis kinetic constant at 350ºC, 385 ºC and 400ºC. Pressure = 25 MPa. Error bars represent the experimental and fitting errors. (***A***) Kinetic constant of glucose isomerization to fructose (triangles) and fructose dehydration (squares) considering OH^- concentration as reagent. (***B***) Kinetic constant of glucose retro aldol condensation (squares), fructose retro aldol condensation (diamonds).

Testing the concept with modified reaction mediums and natural biomass

Finally, in order to test the developments in the kinetics mechanism, fructose was hydrolyzed in modified reactions mediums (with tempo and oxalic acid). On the other hand, wheat bran was hydrolyzed in supercritical water for testing the production of 5-HMF from a natural biomass in supercritical water.

The yields of the main products obtained after fructose hydrolysis are shown in Figure 9. The experiments were carried out in the experimental setup explained above. However, the reaction medium was modified by pumping tempo or oxalic acid. Tempo (2,2,6,6-Tetramethylpiperidin-1-oxyl) is a free radical kidnapper usually employed to control radical reactions in the organic synthesis and polymerization[47]. Oxalic acid was used to increase the concentration of ions in the reaction medium. As it was expected, the production of 5-HMF from fructose at supercritical conditions (400ºC and 23 MPa) was negligible, being pyruvaldehyde the main product after 0.9 s of reaction time. The addition of oxalic acid to the reaction medium increased the availability of protons in the medium, which would promote the fructose dehydration reaction. In fact, when the reaction medium was acidified, the production of 5-HMF in supercritical water was enhanced to 15 % $w \cdot w^{-1}$. The same behavior was observed using tempo as reaction medium modifier. This free radical kidnaper has an acid role due to the dissociation of the OH group bonded to the nitrogen atom. Once again, an acid medium promoted the production of 5-HMF corroborating that 5-HMF production is highly dependent on the protons availability in the medium.

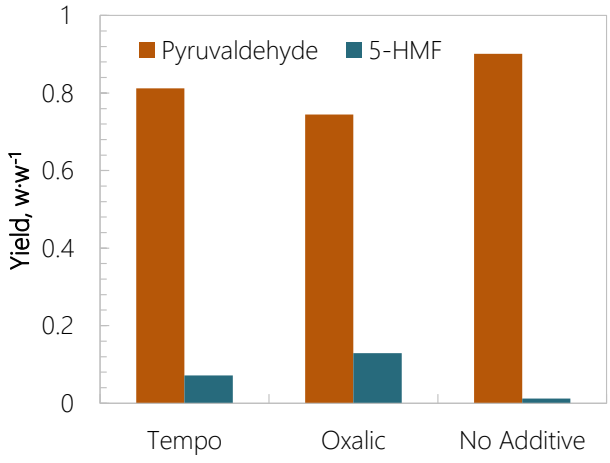

Figure 9. Yields fructose hydrolysis at 400ºC, 23 MPa and 0.9 s of a reaction time. The reaction medium was modified with tempo or oxalic acid.

Wheat bran was also hydrolyzed in the experimental setup aforementioned. The reaction temperature was set at 400ºC with a reactor pressure of 25 MPa. The reaction time was varied from 0.19 s to 0.69 s. Fortunately, as it can be seen in Figure 10, the yields of 5-HMF were lower than 0.05% $w \cdot w^{-1}$. A detailed description of wheat bran hydrolysis for sugars and lignin production can be found in a previous work[48].

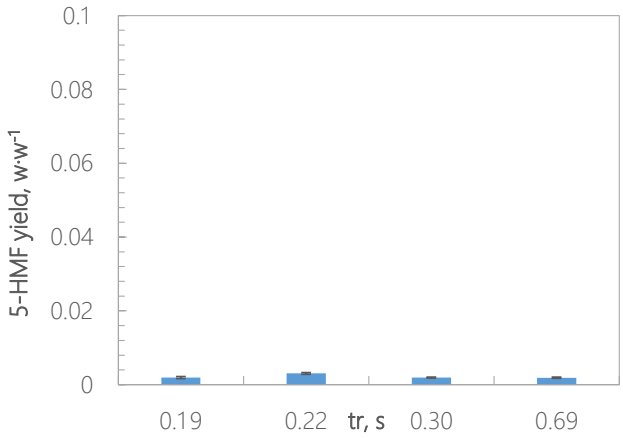

Figure 10. Yields wheat bran hydrolysis at 400ºC and 25 MPa between 0.19 s and 0.69 s of reaction time.

CONCLUSION

The process presented in this work shows an efficient alternative to hydrolyze cellulose selectively. The control of the reaction time is the key to obtain yields higher than 95% $w \cdot w^{-1}$ of soluble sugars or 60% $w \cdot w^{-1}$ of glycolaldehyde. From the viewpoint of chemistry, the selectivity of the process is governed by the ions concentration in the reaction medium. A reaction mechanism model was built and intensively tested to demonstrate its reliability. The reactions of glucose and fructose retro aldol condensation are low demanding of ions. In fact, this reactions are highly improved when the water molecules (reaction medium and reagent) are highly associated. On the other hand, the isomerization reaction of glucose-fructose as well as dehydration reactions of these sugars are extremely diminished when the water molecules are associated. For first time, it was quantitatively explained and demonstrated the

reasons why the production of 5-HMF is highly avoided at supercritical water conditions. It was succeeded by adding the concentration of protons or hydroxide ions due to water dissociation as reagent in the kinetic modelling of the reactions.

The extraordinary changes in the chemical and physical properties of supercritical water allows the biomass hydrolysis choosing the desired products by simply selecting the correct reaction temperature and pressure.

ACKNOWLEDGEMENTS

The authors thank the Spanish Ministry of Economy and Competitiveness for Project CTQ2011-23293, CTQ2011-27347, CQT2013-44143-R and ENE2012-33613. M.D.B thanks the Spanish Ministry of Economy and Competitiveness for Ramón y Cajal research fellowship RYC-2013-13976.

REFERENCES

1. A. J. Ragauskas, C. K. Williams, B. H. Davison, G. Britovsek, J. Cairney, C. A. Eckert, W. J. Frederick, J. P. Hallett, D. J. Leak, C. L. Liotta, J. R. Mielenz, R. Murphy, R. Templer and T. Tschaplinski, *Science*, 2006, **311**, 484 -489.
2. D. Klemm, B. Heublein, H. P. Fink and A. Bohn, *Angewandte Chemie International Edition*, 2005, **44**, 3358-3393.
3. J. Tollefson, *Nature News*, 2008, **451**, 880-883.
4. K. Arai, R. L. Smith Jr and T. M. Aida, *The Journal of Supercritical Fluids*, 2009, **47**, 628-636.
5. K. Barta and P. C. Ford, *Accounts of Chemical Research*, 2014, **47**, 1503-1512.
6. T. M. Aida, Y. Sato, M. Watanabe, K. Tajima, T. Nonaka, H. Hattori and K. Arai, *The Journal of Supercritical Fluids*, 2007, **40**, 381-388.
7. T. M. Aida, K. Tajima, M. Watanabe, Y. Saito, K. Kuroda, T. Nonaka, H. Hattori, R. L. Smith Jr and K. Arai, *The Journal of Supercritical Fluids*, 2007, **42**, 110-119.
8. B. M. Kabyemela, T. Adschiri, R. M. Malaluan and K. Arai, *Industrial & Engineering Chemistry Research*, 1999, **38**, 2888-2895.
9. B. M. Kabyemela, T. Adschiri, R. M. Malaluan, K. Arai and H. Ohzeki, *Industrial & Engineering Chemical Research*, 1997, **36**, 5063-5067.
10. A. Corma, S. Iborra and A. Velty, *Chemical Reviews*, 2007, **107**, 2411-2502.
11. R.-J. van Putten, J. C. van der Waal, E. de Jong, C. B. Rasrendra, H. J. Heeres and J. G. de Vries, *Chemical Reviews*, 2013, **113**, 1499-1597.
12. A. M. Ruppert, K. Weinberg and R. Palkovits, *Angewandte Chemie International Edition*, 2012, **51**, 2564-2601.
13. C. Luo, S. Wang and H. Liu, *Angewandte Chemie International Edition*, 2007, **46**, 7636–7639.

14. L. Shuai and X. Pan, *Energy & Environmental Science*, 2012.
15. C. E. Wyman, B. E. Dale, R. T. Elander, M. Holtzapple, M. R. Ladisch and Y. Y. Lee, *Bioresource Technology*, 2005, **96**, 2026-2032.
16. R. Rinaldi, R. Palkovits and F. Schüth, *Angewandte Chemie International Edition*, 2008, **47**, 8047–8050.
17. S. Morales-delaRosa, J. M. Campos-Martin and J. L. G. Fierro, *Chemical Engineering Journal*, 2012, **181-182**, 538-541.
18. D. A. Cantero, M. D. Bermejo and M. J. Cocero, *The Journal of Supercritical Fluids*, 2013, **75**, 48-57.
19. D. A. Cantero, M. D. Bermejo and M. J. Cocero, *Bioresource Technology*, 2013, **135**, 697-703.
20. D. A. Cantero, M. D. Bermejo and M. J. Cocero, *The Journal of Supercritical Fluids*, 2014.
21. M. Sasaki, T. Adschiri and K. Arai, *AIChE Journal*, 2004, **50**, 192-202.
22. M. Sasaki, B. Kabyemela, R. Malaluan, S. Hirose, N. Takeda, T. Adschiri and K. Arai, *The Journal of Supercritical Fluids*, 1998, **13**, 261-268.
23. M. Sasaki, K. Goto, K. Tajima, T. Adschiri and K. Arai, *Green Chemistry*, 2002, **4**, 285-287.
24. M. Sasaki, Z. Fang, Y. Fukushima, T. Adschiri and K. Arai, *Industrial & Engineering Chemistry Research*, 2000, **39**, 2883-2890.
25. M. J. Antal Jr., W. S. L. Mok and G. N. Richards, *Carbohydrate Research*, 1990, **199**, 91-109.
26. F. S. Asghari and H. Yoshida, *Ind. Eng. Chem. Res.*, 2007, **46**, 7703-7710.
27. F. S. Asghari and H. Yoshida, *Carbohydrate Research*, 2010, **345**, 124-131.

28. M. Bicker, D. Kaiser, L. Ott and H. Vogel, *The Journal of Supercritical Fluids*, 2005, **36**, 118-126.
29. D. Bröll, C. Kaul, A. Krämer, P. Krammer, T. Richter, M. Jung, H. Vogel and P. Zehner, *Angewandte Chemie International Edition*, 1999, **38**, 2998–3014.
30. V. Choudhary, S. H. Mushrif, C. Ho, A. Anderko, V. Nikolakis, N. S. Marinkovic, A. I. Frenkel, S. I. Sandler and D. G. Vlachos, *Journal of the American Chemical Society*, 2013, **135**, 3997-4006.
31. K. Ehara and S. Saka, *Journal of Wood Science*, 2005, **51**, 148-153.
32. F. Jin, Z. Zhou, T. Moriya, H. Kishida, H. Higashijima and H. Enomoto, *Environ. Sci. Technol.*, 2005, **39**, 1893-1902.
33. D. Klingler and H. Vogel, *The Journal of Supercritical Fluids*, 2010, **55**, 259-270.
34. X. Lü and S. Saka, *The Journal of Supercritical Fluids*, 2012, **61**, 146-156.
35. T. Sakaki, M. Shibata, T. Miki, H. Hirosue and N. Hayashi, *Energy & Fuels*, 1996, **10**, 684-688.
36. M. Akizuki, T. Fujii, R. Hayashi and Y. Oshima, *Journal of Bioscience and Bioengineering*.
37. Wagner, W, Cooper, R. J, Dittmann, A, Kijima, J, Kretzschmar, J. H, Kruse, Mares, R, Oguchi, K, Sato, H, St, Cker, I, Sifner, O, Takaishi, Y, Tanishita, Tr, Benbach, Willkommen and G. T, American Society of Mechanical Engineers, New York, N, ETATS-UNIS, 2000.
38. W. L. Marshall and E. U. Franck, *Journal of Physical and Chemical Reference Data*, 1981, **10**, 295-304.
39. N. Akiya and P. E. Savage, *Chemical Reviews*, 2002, **102**, 2725-2750.
40. A. Kruse and A. Gawlik, *Industrial & Engineering Chemistry Research*, 2002, **42**, 267-279.

41. H. Weingärtner and E. U. Franck, *Angewandte Chemie International Edition*, 2005, **44**, 2672–2692.
42. C. Promdej and Y. Matsumura, *Industrial & Engineering Chemistry Research*, 2011, **50**, 8492-8497.
43. R. S. Assary, T. Kim, J. J. Low, J. Greeley and L. A. Curtiss, *Physical Chemistry Chemical Physics*, 2012, **14**, 16603-16611.
44. Y. Zhao, W.-J. Lu and H.-T. Wang, *Chemical Engineering Journal*, 2009, **150**, 411-417.
45. S. Kumar and R. B. Gupta, *Industrial & Engineering Chemistry Research*, 2008, **47**, 9321-9329.
46. C. Schacht, C. Zetzl and G. Brunner, *The Journal of Supercritical Fluids*, 2008, **46**, 299-321.
47. C. J. Hawker, *Accounts of Chemical Research*, 1997, **30**, 373-382.
48. D. A. Cantero, C. Martinez, M. D. Bermejo and M. J. Cocero, *Green Chemistry*, 2015.